Journal of Soil Science and Plant Nutrition (2026) 26:3910–3924
https://doi.org/10.1007/s42729-026-03106-x

ORIGINAL PAPER

From Soil To Solution: Metabolomic and Antimicrobial Insights into *Acorus Calamus* L. Root Systems

Andrew D'Souza[1] · Kannath U. Sanjay[1] · Neeharika Narisepalli Venkatasai[1] · Padmalatha S. Rai[1]

Received: 16 October 2025 / Accepted: 27 January 2026 / Published online: 20 February 2026
© The Author(s) 2026

Abstract
Acorus calamus L. (*A. calamus*) is a valuable medicinal plant traditionally used in Indian medicine for its therapeutic rhizomes. However, overharvesting has endangered natural populations, highlighting the need for alternative plant parts and sustainable cultivation methods. This study aimed to evaluate hydroponic cultivation as a sustainable strategy and to compare the metabolite and antibacterial profiles of hydroponically grown *A. calamus* roots with those of soil-grown rhizomes. Plants were cultivated using both hydroponic and soil-based systems. Growth performance was assessed, followed by LC-MS-based metabolomic profiling to identify key bioactive compounds. Network pharmacology analysis was used to predict antibacterial targets. The antibacterial activity of the root extracts was evaluated against *Pseudomonas aeruginosa*, *Enterococcus faecalis*, *Staphylococcus aureus*, and *Streptococcus mutans.* Hydroponically grown plants showed enhanced growth, including greater root biomass, compared to soil-grown plants. LC-MS analysis revealed higher concentrations of key bioactive metabolites, including allantoin, graveoline, and capnoidine, in hydroponic roots. Network pharmacology identified key antibacterial targets, including TLR4, TNF, BCL2, and HSP90AA1. Antibacterial assays demonstrated that hydroponic root extracts effectively inhibited the tested bacterial strains, with activity comparable to that of soil-grown roots. Our findings showed that hydroponic cultivation could effectively produce *A. calamus* roots with enhanced metabolite content and antibacterial efficacy. This approach offers a sustainable and effective method for utilising *A. calamus* roots as a reliable alternative for wild rhizomes.

Keywords Acorus calamus · Antibacterial activity · Hydroponic cultivation · Metabolomics · Network pharmacology

1 Introduction

Medicinal plants are vital sources of bioactive compounds that possess therapeutic potential for diverse disease conditions. They remain an integral part of traditional Indian medicinal systems, including Ayurveda, Unani, and Siddha, among others (Prasathkumar et al. 2021). *Acorus calamus* L., a member of the family Acoraceae and commonly known as sweet flag, is a perennial herb with significant medicinal value. The rhizome of *A. calamus* has long been used in traditional medicine to manage various conditions, including neurological, digestive, respiratory, psychological, cognitive, dermatological, and vascular disorders (Rajput et al. 2014; He et al. 2023). The therapeutic properties of this plant arise from its rich array of secondary metabolites, which not only support its growth and development but also exhibit antibacterial properties (Haran et al. 2024). The rising demand for medicinal herbs has created a critical sustainable crisis. Several plant species are at risk of extinction due to intensive harvesting practices and limitations in conventional farming methods, including soil erosion, declining soil fertility, climate variability, and water scarcity (Kaur and Dewan 2023; Regmi and Neupane 2023). Thus, there is a pressing need for sustainable and efficient cultivation practices to mitigate these challenges. Hydroponics, a cultivation technique that eliminates soil dependency by growing plants in a nutrient-rich solution, offers one such transformative approach. In this system, plants can be cultivated directly in the nutrient solution or in an inert growing medium such as clay, pebbles, or coconut coir, which provides root support while maintaining optimal nutrient

✉ Padmalatha S. Rai
padmalatha.rai@manipal.edu

[1] Department of Biotechnology, Manipal School of Life Sciences, Manipal Academy of Higher Education, Manipal 576104, India

delivery (Atherton and Li 2023). Hydroponics are increasingly popular due to their numerous advantages, including eliminating the need for soil, efficient use of space, faster growth rates, shorter harvesting cycles, and reduced risk of pests and diseases. To date, no comparative research has assessed differences in growth dynamics, photosynthetic efficiency, and metabolite profiles between *A. calamus* roots grown in soil and in hydroponic systems. Moreover, while most pharmacological studies on *A. calamus* have primarily focused on its rhizome, the root system remains an underexplored reservoir of potentially bioactive secondary metabolites. Here, we hypothesize that hydroponically grown roots of *A. calamus* could serve as an alternative source of therapeutically relevant secondary metabolites, comparable to those obtained from conventionally soil-grown rhizomes. Accordingly, this study aims to investigate and characterise cultivation-induced variations in metabolite composition, photosynthetic performance, and plant growth, and to identify bioactive compounds with potential antibacterial activity and therapeutic relevance. By integrating physiological, metabolomic, antibacterial, and computational analyses, this work offers novel insights into the bioactive potential of the roots and underscores hydroponics as a sustainable approach for cultivating medicinal plants.

2 Methodology

2.1 Plant Collection and Molecular Identification of *A. Calamus*

Six accessions of *A. calamus* were collected from Manipal, Karnataka, India. The herbarium voucher specimen was identified with the help of a taxonomist, and the *A. calamus* germplasm was preserved in the greenhouse at the Manipal School of Life Sciences, Manipal Academy of Higher Education, Manipal, India. Genomic DNA isolation from *A. calamus*. was performed using a modified CTAB-based method (Tiwari et al. 2012). Molecular identification was performed using the *nrITS* marker. The amplified products were analysed on a 1.2% agarose gel and then subjected to Sanger sequencing using the Genetic Analyser 3500. The sequence obtained was submitted to GenBank.

2.2 Cultivation Method

For plant cultivation, 10-inch plastic pots were used to grow *A. calamus*, and greenhouse soil was used. Plants were monitored and watered regularly over a six-week period. The hydroponic setup was arranged in the institute's hydroponics lab. The system consisted of a 5-litre plastic tub, netted pots, and an air pump. 4-inch holes spaced 10 cm apart were drilled in the lid of the plastic tub to fit the 6-inch netted pots. Initially, six rhizomes were planted in soil pots; later, three rhizomes were planted in a hydroponics system and allowed to establish. They were acclimatised by placing them in half-strength Hoagland nutrient solution within the netted pots. A full-strength Hoagland solution was used to grow the plants, maintaining an electrical conductivity (EC) of 1.5–2.5 mS/cm and a pH of 5.5–6.5. The nutrient solution was replaced every week, and an air pump was used to aerate the tub. The system was maintained in a controlled environment at 30 °C for over six weeks to ensure optimal growth conditions. The roots of *A. calamus from* each group (three plants pooled per group) were frozen in liquid nitrogen and stored at −20 °C for further use.

2.3 Growth and Gas Exchange Parameters

Growth parameters, including shoot height, leaf number, and root length, were determined quantitatively using a ruler for height measurements and manual leaf counts, respectively. Following harvest, the biomass of *A. calamus* root was determined by weighing. Gas exchange measurements were conducted using the LICOR 6400 XT portable photosynthetic system (LICOR Inc., Lincoln, NE, USA) within the greenhouse between 10:00 AM and 11:00 AM. Measurements were recorded at 2, 4, and 6 weeks during the six-week experimental timeline. The leaf chamber environment was maintained at 400 mg kg^{-1} CO_2, with an artificial light source providing photosynthetically active radiation (PAR) at an intensity of 500 µmol s^{-1} m^{-2}. Key physiological parameters, including net photosynthetic rate, transpiration rate, stomatal conductance, and intercellular CO2 concentration, were assessed (Thorat et al. 2024). A student's t-test was used to determine the statistical significance between the two groups.

2.4 Metabolite Fingerprinting

The root samples of *A. calamus* obtained from each group (soil and hydroponics) were used for untargeted metabolite profiling. 100 mg of the powdered sample was used to prepare methanolic extracts as mentioned in De Vos et al. 2007 (De Vos et al. 2007). A QExactive Orbitrap high-resolution mass spectrometer, coupled with a Vanquish UHPLC system (Thermo Fisher Scientific, Inc., USA), was used for LC-MS analysis. The solvent conditions, gradient program, and other parameters were set as described by Vinay et al. (2025). The raw mass spectrometry file was generated using Thermo Xcalibur 2.0 software. Compound-discovery software was used to identify metabolites. Untargeted metabolomics, utilising online databases, mzLogic, and a molecular networks workflow, was employed for compound annotation.

2.5 Statistical Analysis

Statistical analysis of the annotated metabolites was conducted using MetaboAnalyst 6.0 (Pang et al. 2024). Principal component analysis (PCA) and orthogonal partial least squares discriminant analysis (OPLS-DA) were conducted to assess the variation between the two groups. A Student's t-test with p-value < 0.05 was used to identify statistically significant metabolites. The VIP score from the OPLS-DA model was used to identify metabolites contributing to group separation.

2.6 Target Prediction and protein-protein Interaction (PPI) Network Construction

The annotated compounds were filtered to focus exclusively on secondary metabolites derived from plants. The target genes associated with these metabolites were predicted using Swiss Target Prediction (Jilani and Packirisamy 2024), with genes having a probability score of 0.1 or higher included. These targets were then cross-referenced with a list of antibacterial targets retrieved from the GeneCards database (Kim et al. 2024), selecting those with a relevance score greater than 0.7. The targets shared by both sets were identified, and a PPI network was generated for the shared targets, utilising a confidence score threshold of 0.8 in StringDB (Cytoscape v3.10.2). To identify the top ten hub targets, the Cyto-Hubba plugin was used (Sahu et al. 2024; Szklarczyk et al. 2019).

2.7 Ligand and Protein Preparation

The 3D structure minimisation of the secondary metabolites was performed using LigPrep Tool (Schrodinger 2021-2, LLC, New York). The crystal structures of the hub targets were retrieved from the Protein Data Bank and the AlphaFold databases (Burley et al. 2021; Jumper et al. 2021). Among these, the structures with higher resolution, obtained via X-ray crystallography, were chosen, along with detailed positional data for each target.

2.8 ADME Analysis Using QikProp

The ADMET properties of the target structures were assessed using the QikProp module in Schrodinger software (schrodinger.com). The analysis focused on several key parameters, including the predicted octanol/water partition coefficient (–2.0–6.5), aqueous solubility (–6.5–0.5), IC50 value for HERG K+ channel inhibition (concern for values below −5), predicted permeability in Caco-2 cells (nm/sec) (<25-poor, >500-great), human oral absorption (percentage scale) (>80%-high, <25%-poor) (Percent Human Oral Absorption), Van der Waals surface area for polar nitrogen, oxygen, and carbonyl carbon atoms (7.0–200.0) (PSA), and adherence to Lipinski's rule of five (=0). Molecular docking studies were then performed on the selected structures (Liu et al. 2020).

2.9 Molecular Docking

Molecular docking was performed using Schrodinger Suite. The Glide-Receptor Grid generation module was used to generate the grid, while the SiteMap module was used to identify ligand-binding sites on hub targets. Extra precision docking was performed using Glide, and the resulting docked conformations were evaluated based on their GlideScore (G-score) to estimate binding affinity and rank potential interactions (Kontoyianni 2017).

2.10 Antibacterial Assay

The antibacterial properties of the DMSO extract of *A. calamus* were assessed using the agar well diffusion method, with slight modifications based on the procedure outlined by Haran et al. (2024). Mueller Hinton agar plates were sterilised by autoclaving at 121 °C for 15–20 min (Haran et al. 2024). The agar was poured into 10 cm petri dishes, and bacterial cultures of *Pseudomonas aeruginosa* (ATCC 27853), *Enterococcus faecalis* (ATCC 29212), *Staphylococcus aureus* (ATCC 29213), and *Streptococcus mutans* (ATCC 25175) were prepared in Mueller-Hinton broth. These bacterial suspensions were evenly spread across the agar surface using a sterile cotton swab. Wells were created in the agar using a sterile polystyrene tip and filled with 2000 µg of the extract. A 250 µg/ml solution of Ciprofloxacin was used as the positive control, and 10% DMSO served as the negative control. The plates were incubated at 37 °C for 24 and 48 h. Antibacterial activity was evaluated by measuring the diameter of the inhibition zones around the wells, recorded in millimetres (mm) with a stencil in triplicate. The size of these inhibition zones indicated the plant extract's antibacterial activity.

3 Results

3.1 Sample Collection and Molecular Identification of *A. Calamus*

A fresh sample of *A. calamus* was collected from Karnataka, India. The herbarium voucher specimen was taxonomically identified by a taxonomist, and the germplasm was preserved in the greenhouse. Molecular authentication of *A. calamus* was carried out using the *nrITS* marker. The amplified DNA region

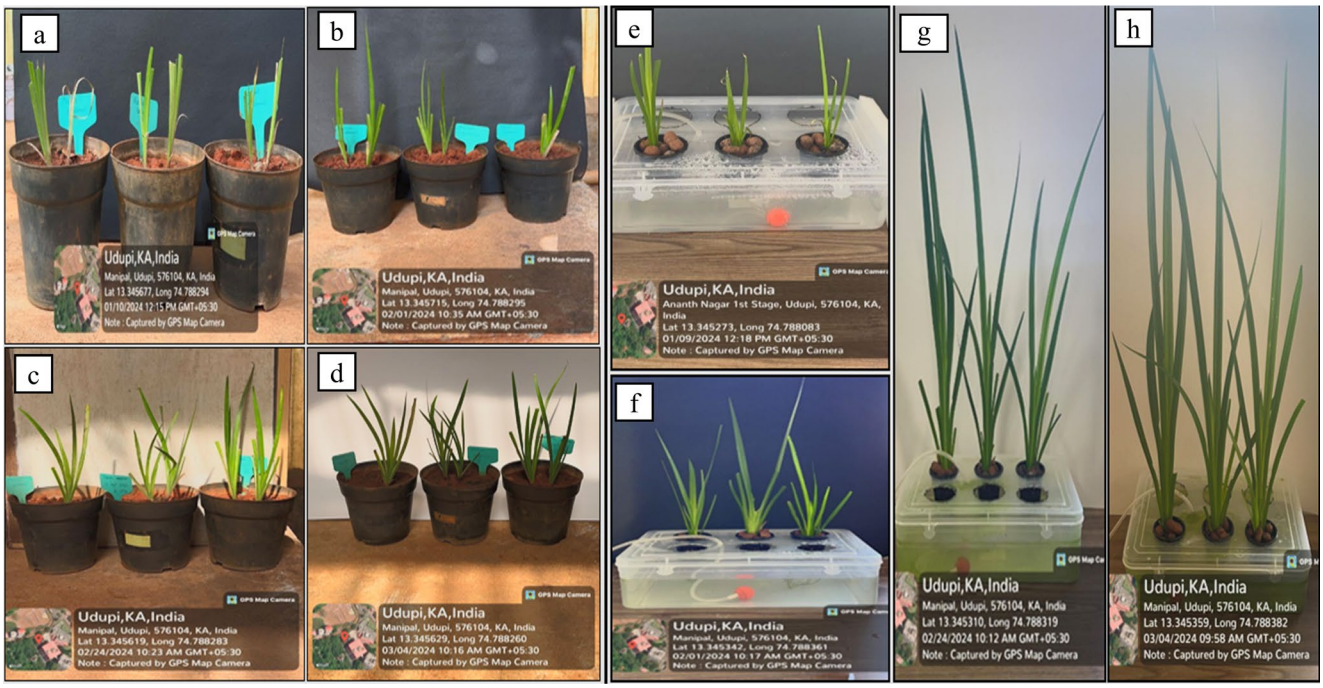


Fig. 1 *A. calamus* grown in soil and hydroponic conditions: (**a**) Soil grown at week zero, (**b**) Soil grown at week two, (**c**) Soil grown at week four, (**d**) Soil grown at week six, (**e**) Hydroponically grown at week zero, (**f**) Hydroponically grown at week two, (**g**) Hydroponically grown at week four, (**h**) Hydroponically grown at week six

Table 1 Growth parameters of *A. calamus* grown in hydroponics vs. soil-based cultivation

Growth parameters	Days	Hydroponics	Soil	df	Significance
Plant height (cm)	0	10	10		
	14	27±2.6	14±1	4	<0.01**
	28	47.6±2.5	16.3±1.5	4	<0.001***
	42	57.6±2.5	23.3±1.5	4	<0.001***
Number of leaflets	0	5±1	5.3±0.57	4	>0.05
	14	5.6±0.5	6.3±2.08	4	>0.05
	28	6.6±1.15	7±1.73	4	>0.05
	42	7.3±0.5	8±1.73	4	>0.05
Initial fresh weight of the root (g)	0	NA	NA	4	
Fresh weight of the root (g)	42	3.8±0.95	0.74±0.66	4	<0.05*
Dry weight of the root (g)	42	0.68±0.11	0.2±0.135	4	<0.05*

All values are represented as (mean±SD); *: $p<0.05$, **: $p<0.01$, ***:$p<0.001$

SA Salicylic acid; *df* Degrees of freedom; *NA* Not applicable (Rhizome was cultivated without roots)

was subjected to DNA Sanger sequencing, and the sequence was submitted to NCBI GenBank (Accession No. PP818955).

3.2 Cultivation of *A. Calamus* and its Growth Parameters

The *A. calamus* rhizomes were grown in both soil and hydroponic systems for six weeks (Fig. 1). Growth parameters, such as plant height and leaf number, were measured at the beginning of the study and at two-week intervals until the end of the six-week period in both systems. Root biomass was measured at the end of a six-week period. In the hydroponic system, there was a significant increase (2.45-fold) in plant height compared to the plants grown in soil. The number of leaves on hydroponically grown plants showed a slight decrease (0.9125-fold) compared with those grown in soil. However, the root biomass of the hydroponically grown *A. calamus* showed a significant increase (5-fold) over that of the soil-grown plants (Table 1).

3.3 Gas Exchange Parameters of *A. Calamus*

Gas exchange measurements, including photosynthetic rate, stomatal conductance, transpiration rate, and internal

carbon dioxide concentration, were recorded throughout the cultivation period for *A. calamus* grown in both soil and hydroponic systems, revealing distinct phases in photosynthetic rates. A notable increase in the net photosynthetic rate occurred between weeks 2 and 4, indicating a transition toward peak photosynthetic activity, followed by a decrease as the plants approached maturity by week 6. In the hydroponic system, stomatal conductance and transpiration rate displayed a two-phase pattern, with a reduction by week four and an increase by week six, suggesting adaptive responses to environmental or developmental factors. Similarly, internal CO_2 concentration decreased slightly at week four before moderately increasing by week six, reflecting possible adjustments in carbon assimilation efficiency (Fig. 2).

Gas exchange measurements, including photosynthetic rate, stomatal conductance, transpiration rate, and internal carbon dioxide concentration, were recorded throughout the cultivation period for *A. calamus* grown in both soil and hydroponic systems. In hydroponically grown plants, the photosynthetic rate increased by one-fold at week two compared to soil-grown plants. This was followed by a significant 9-fold increase at week four. However, by the end of the six-week period, the photosynthetic rate decreased by 2.08-fold relative to soil-grown plants.

The internal CO_2 concentration in hydroponically grown plants initially increased by 1-fold. It then decreased by 0.83-fold at the end of week four and increased again by one-fold by the end of six weeks. Stomatal conductance showed a steady upward trend in hydroponically grown plants, increasing 2-fold at week two, 1.4-fold at week four, and reaching 2.84-fold by the end of the cultivation period. The transpiration rate followed a pattern similar to stomatal conductance, reflecting the overall improvement in gas exchange under hydroponic conditions.

3.4 Metabolite Profiling of *A. Calamus* Grown in Soil and Hydroponic Cultivation Systems

Untargeted metabolite profiling of *A. calamus* grown in soil and hydroponic conditions has identified 6674 and 5846 metabolite features, respectively. The t-test analysis of 143 annotated common metabolites identified 35 statistically significant metabolites (p-value < 0.05) (Table 2). Among these, allantoin, daucic acid, pseudouridine, acaciabiuronic acid, and 1-aminocyclopropane-1-carboxylate showed the highest statistical significance at the 95% confidence level (Fig. 3A). The unsupervised PCA plot revealed a clear separation between the soil and hydroponics groups. PC1 accounted for 37.1% of the total variation, PC2 accounted for 18.9%, and PC3 accounted for 16.9%, collectively

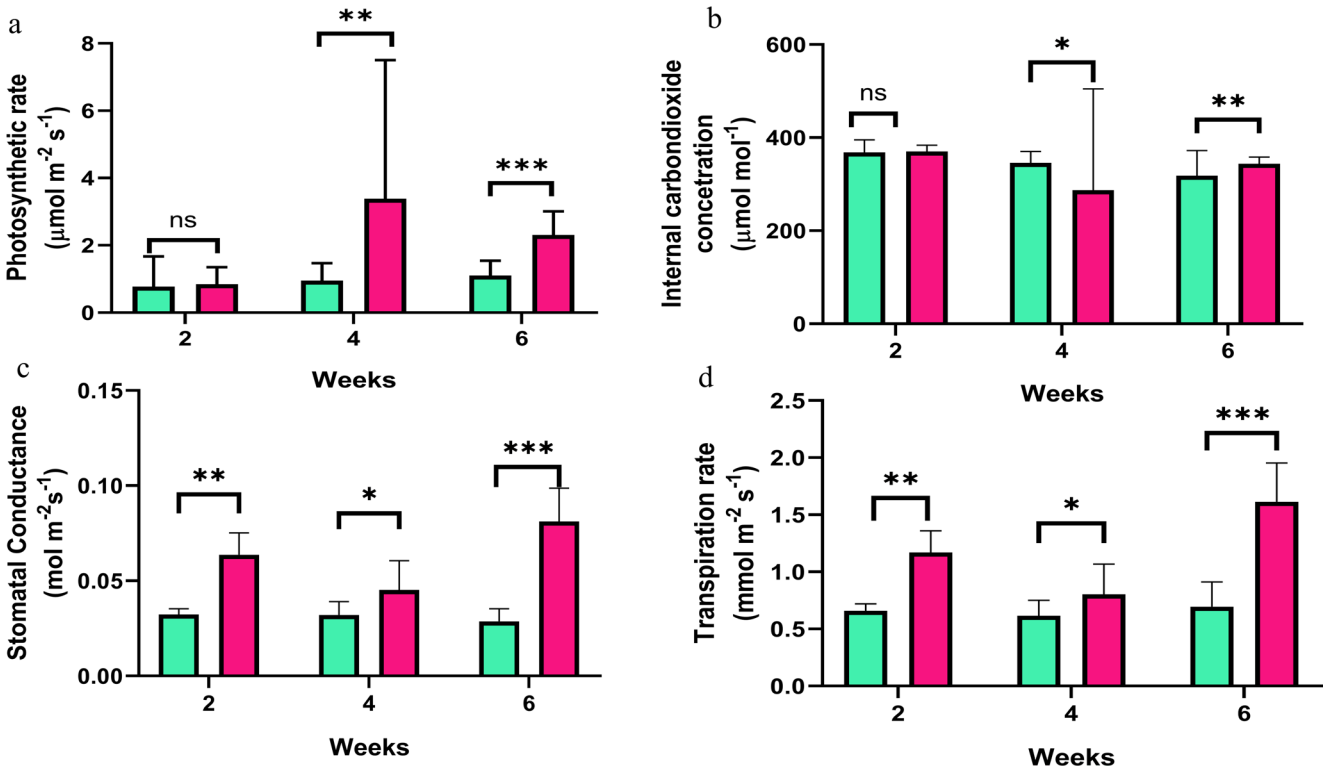


Fig. 2 Graphical representation of gas exchange parameters: (**a**) Photosynthesis rate, (**b**) Internal Carbon dioxide concentration, (**c**) Stomatal conductance, (**d**) Transpiration rate

Table 2 List of statistically significant plant metabolites present in *A. calamus* in both hydroponics and soil systems

Plant Metabolites	M/z value	Retention time	Adduct
Allantoin	157.036	4.935	[M-H]−1
Pseudouridine	243.062	15.409	[M-H]−1
Daucic acid	203.019	12.681	[M-H]−1
Acaciabiuronic acid	355.088	4.977	[M-H]−1
1-Aminocyclopropane-1-carboxylate	102.055	4.288	[M+H]+1
(2R,3R)−3-Methylornithine	147.113	3.333	[M+H]+1
Proline betaine	144.102	5.399	[M+H]+1
Glaziovine	298.143	18.621	[M+H]+1
3-(Pyrazol-1-yl)-L-alanine	154.061	3.498	[M-H]−1
Methyl 2-furoate	127.039	4.612	[M+H]+1
Capnoidine	387.114	4.939	[M+FA-H]−1
4-Guanidinobutanoic acid	146.092	5.424	[M+H]+1
1,3,5-Trihydroxy-10-methylacridone	256.059	4.767	[M-H]−1
Graveolinine	299.098	5.204	[M+FA-H]−1
sn-Glycero-3-phosphocholine	281.099	19.516	[M+Na]+1
D-serine and L-serine	104.034	4.118	[M-H]−1
Acetamidopropanal	116.071	3.528	M+H]+1
D-Xylitol	151.06	4.581	[M-H]−1
2-Furancarboxaldehyde	97.029	4.611	[M+H]+1
Inosine	267.072	5.699	[M-H]−1
Ribose-1-arsenate	272.959	2.966	[M+NH4]+1
3,5-Dihydroxyphenyl 1-O-(6-O-galloyl-beta-D-glucopyranoside)	439.086	5.342	[M-H]−1
Pinidine	157.17	3.117	[M+NH4]+1
4-Aminobutyric acid	104.071	3.821	[M+H]+1
Indole	118.065	19.296	[M+H]+1
(3Z)-Phytochromobilin	293.143	21.887	[M+2 H]+2
Thymine	125.034	4.269	[M-H]−1
6-(5-carboxy-2,3-dihydroxyphenoxy)−3,4,5-trihydroxyoxane-2-carboxylic acid	381.027	4.272	[M+Cl]−1
Triphenyl phosphate	327.075	22.137	[M+H]+1
N-Phenylacetylaspartic acid	250.072	21.961	[M-H]−1
Lucidenic acid A	481.261	21.342	[M+Na]+1
1'-Acetoxyeugenol acetate	265.104	22.137	[M+H]+1
4-Hydroxycitrulline	174.087	5.448	[M+H-H2O]+1
2-Hydroxymethylserine	134.046	7.949	[M-H]−1
Camelledionol	221.17	16.595	[M+2 H]+2

explaining 72.9% of the observed variation (Fig. 3B). Similarly, the OPLS-DA plot also showed a clear separation between soil and hydroponic systems, with a T score of 42.9% and an orthogonal T score of 16.7%. OPLS-DA model with R2X = 0.49, R2Y = 0.984 and Q2 = 0.858, indicating that it is a good model (Fig. 4). A hierarchical clustering heatmap revealed that graveoline, capnoidine, and allantoin were upregulated in the hydroponic system, while ribose-1-arsenate, daucic acid, and glaziovine were upregulated in soil-grown plants (Fig. 5A). Variable importance in projection (VIP) scores from OPLS-DA highlighted key metabolites, such as graveoline, capnoidine, and allantoin, which contributed to the separation of the groups (soil and hydroponics) (Fig. 5B).

3.5 Prediction of Antibacterial Secondary Plant Metabolite targets, protein-protein Interaction Network Analysis

The targets of annotated plant secondary metabolites were identified using Swiss Target Prediction, while GeneCards was utilised to retrieve antibacterial targets. A comparative analysis revealed 45 overlapping targets between the antibacterial targets ($n = 354$) and the predicted targets ($n = 434$). A PPI network was constructed by integrating the interactions between predicted and antibacterial targets using Cytoscape. The resulting network comprised 45 nodes and 87 edges, representing interactions between the identified targets (Fig. 6A). Hub targets were identified based on degree, with the top 10 nodes (each with a degree greater than 8) chosen as key hub targets. These included TLR4, TNF, BCL2, HSP90AA1, NFKB1, CASP3, MTOR, ICAM1, IKBKB, and CASP1. The nodes were visualised using a colour gradient, with red indicating the highest degree values and yellow indicating lower values (Fig. 6B).

3.6 Molecular Docking

The binding modes of the 59 ligands with 10 hub proteins were analysed, revealing strong binding affinities with TNF (−12.94 Kcal/mol), MTOR (−11.6 Kcal/mol), and ICAM1 (−10.51 Kcal/mol), while BCL2 showed the least binding affinity (−6.052 Kcal/mol). The extra-precise molecular docking results, including docking scores, for the top ligands against the hub targets, are shown in Table 3.

3.7 Antibacterial Assay by Agar Disc Diffusion Method

The DMSO extract of *A. calamus* demonstrated significant antibacterial activity against *P. aeruginosa*, *S. aureus*, *S. mutans*, and *E. faecalis*, as evidenced by the formation of clear inhibition zones. The inhibition zone diameters for *P. aeruginosa* ranged from 25 to 30 mm for soil-grown plants and 24–30 mm for hydroponically grown plants. Similarly, for *S. aureus*, inhibition zones ranged from 15 to 22 mm for soil-grown plants and 14–19 mm for hydroponically grown plants. Against *S. mutans*, the zones of inhibition were

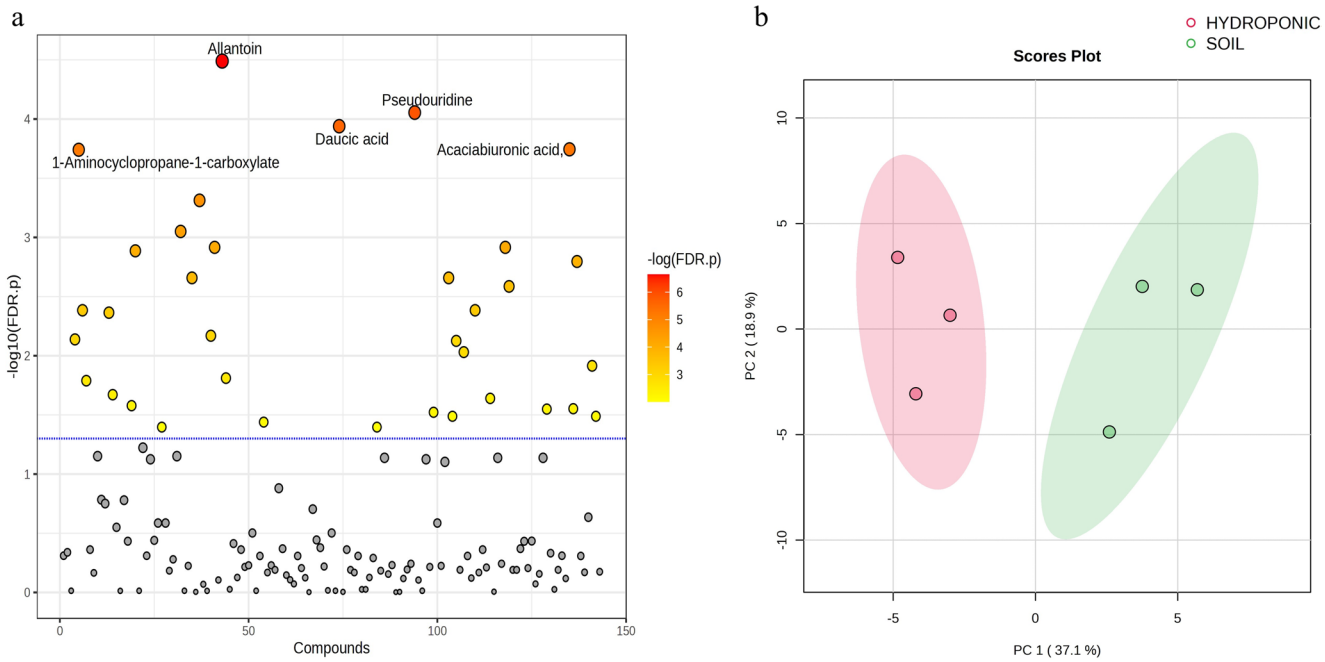


Fig. 3 (**a**)Two-sample t-test analysis of plant metabolites from *A. calamus* grown in hydroponics and soil-based cultivation, (**b**) Principal component analysis (PCA) 2D score plot for soil vs. hydroponics

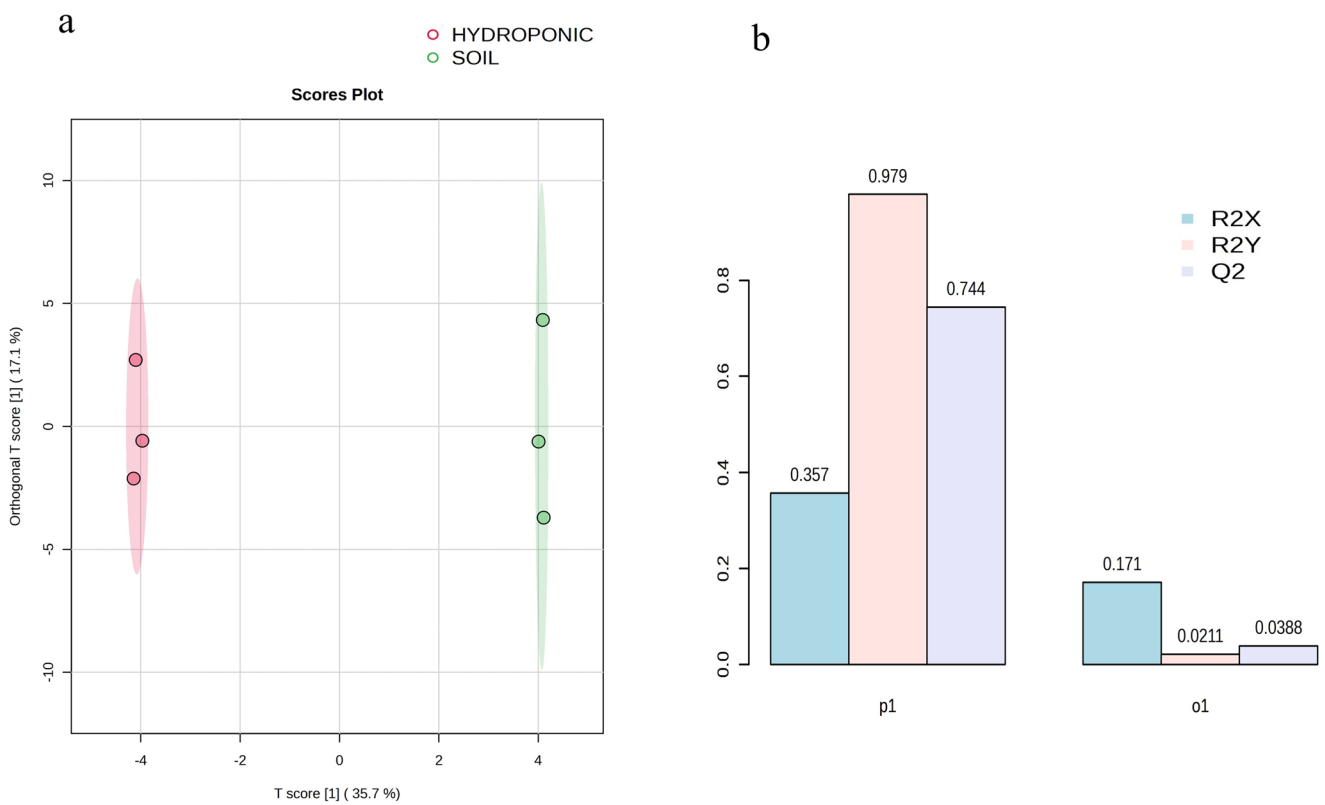


Fig. 4 (**a**) Orthogonal partial least squares discriminant analysis (OPLS-DA) 2D score plot, (**b**) OPLS-DA model overview for soil vs. hydroponics

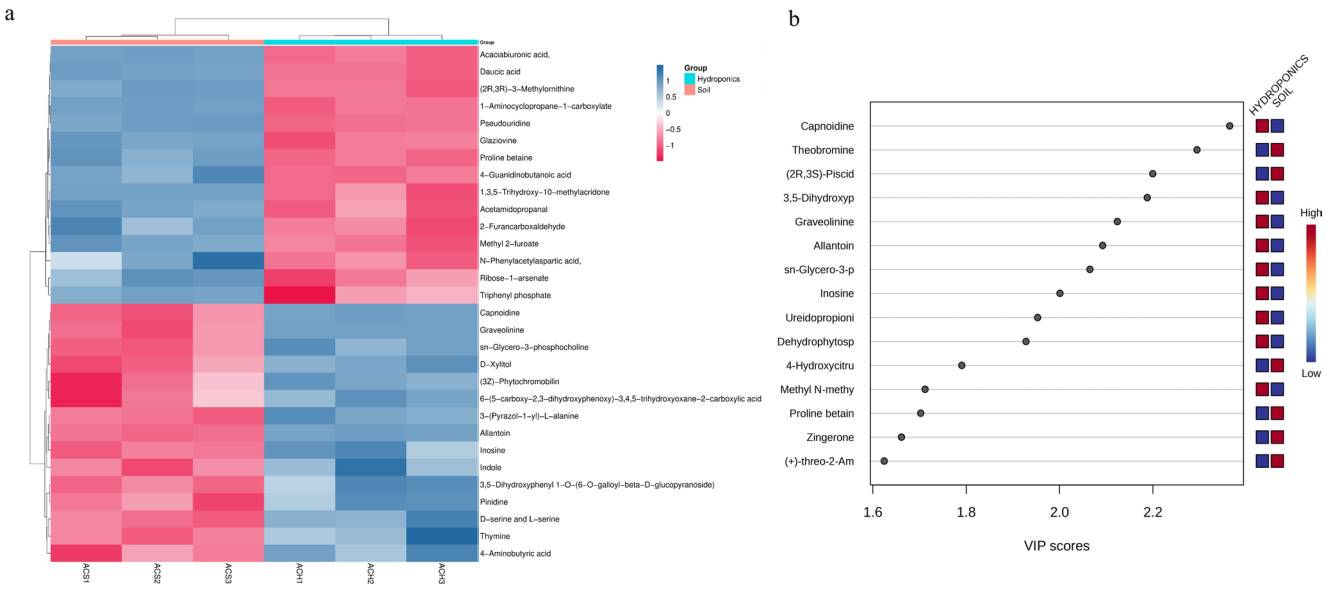


Fig. 5 (**a**) Heat map representing differentially expressed metabolites in soil and hydroponically grown *A. calamus*, (**b**) Variable Importance in Projection (VIP) scores obtained from OPLS-DA analysis by comparing metabolite profiles of *A. calamus* grown under soil and hydroponic conditions

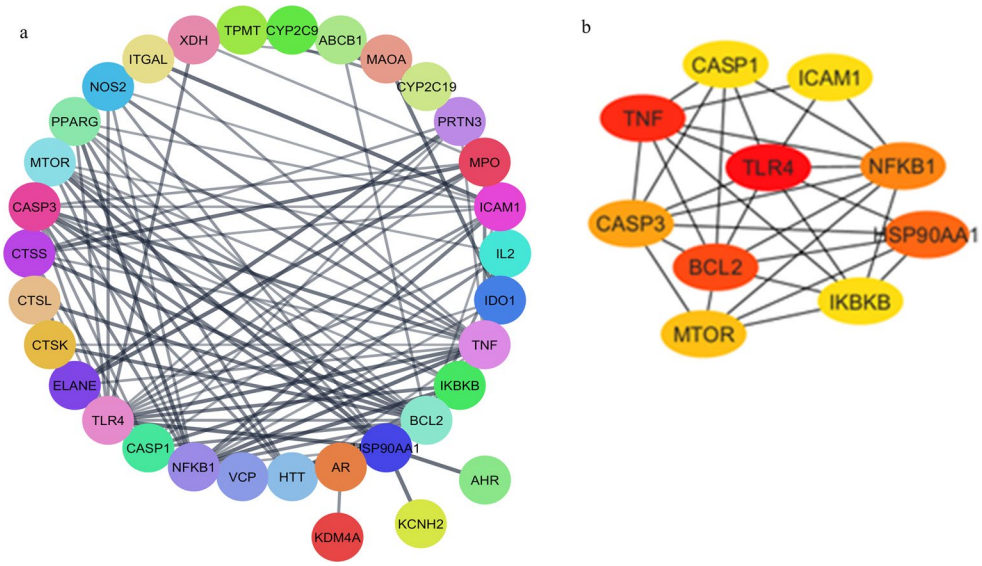


Fig. 6 (**a**) Protein-protein interaction network of the predicted targets and the antibacterial targets, (**b**) Identified top ten hub targets

15–19 mm for soil cultivation and 14–20 mm for hydroponic cultivation. For *E. faecalis*, inhibition zones ranged from 16 to 17 mm in soil-grown plants and 18–19 mm in hydroponically grown plants. A t-test was used to determine the statistical significance between the extracts (soil and hydroponics) and the positive control. The inhibition zones for both the soil and hydroponic extracts were significant against *E. faecalis* (Table 4). Additionally, the hydroponic root extract demonstrated antibacterial properties comparable to those of Ciprofloxacin against *P. aeruginosa*, *S. aureus*, *and S. mutans* (Fig. 7).

4 Discussion

Hydroponic cultivation of therapeutic plants offers solutions to challenges such as soil-borne diseases, water scarcity, and limited fertile land. However, the effects of different cultivation methods on the physiological traits and metabolite profiles of *A. calamus* remain largely unexplored. This study compares the physiological parameters, such as growth and gas exchange, along with metabolomic profiles and antimicrobial activity of *A. calamus* grown in hydroponic versus traditional soil-based systems. While most pharmacological

Table 3 Summary of glide score, non-bonded interactions and 2D interaction diagram of the selected hub genes for the top ligands

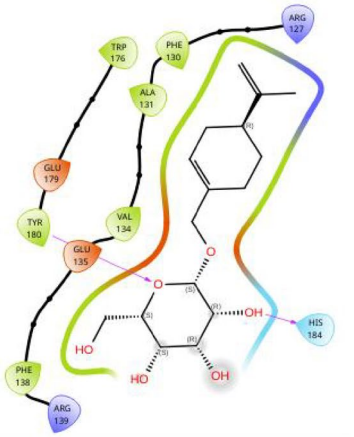
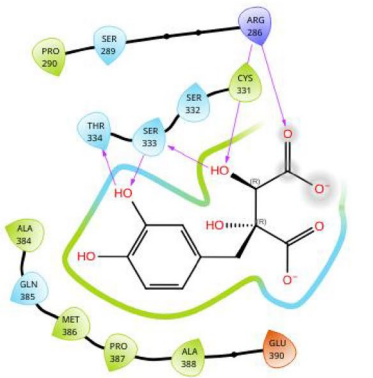
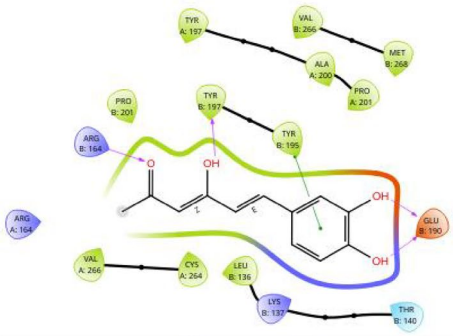
Compound (PubChem ID)	Docking score	Glide emodel	Hub targets	Non-bonding interaction	Interaction diagram
Stachydrine (115244)	-5.745	-39.110	BCL2	H bond: TYR 180, HIS 184 Polar: HIS 184 Charged positive: ARG 127, ARG 139 Charged negative: GLU 135, GLU 179 Hydrophobic: PHE 130, ALA 131, VAL 134, PHE 138, TRP 176, TYR 180	
Lathyrine (166766)	-7.735	-34.029	CASP1	H bond: ARG 286, SER 333,THR 334 Polar: SER 289, SER 332, SER 333, THR 334, GLN 385 Charged positive: ARG 286 Charged negative: GLU 390 Hydrophobic: PRO 290, CYS 331, ALA 384, MET 386, PRO 387, ALA 388	
Lathyrine (166766)	-10.611	-29.403	CASP3	H bond: ARG B:164,TYR B:197, GLU B:190 Pi-Pi stacking: TYR B:195 Polar: THR B:140 Charged positive: LYS B:137,ARG A:164, ARG B:164 Charged negative: GLU B:190 Hydrophobic :LEU B:136, CYS A:264, VAL A:266, TYR B:195, TYR B:197, PRO A:201, PRO B:201, ALA A:200, TYR A:197, MET B:268, VAL B:266	

Table 3 (continued)

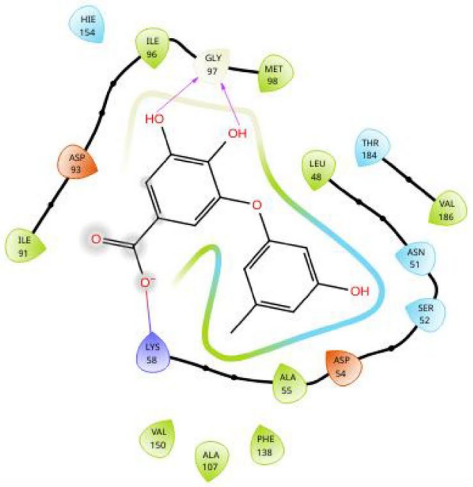
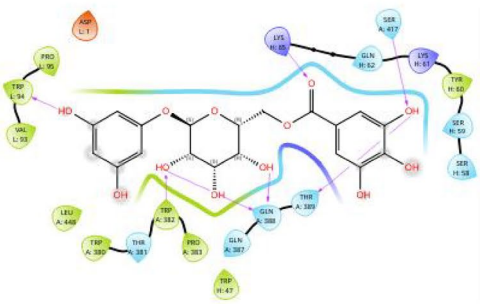
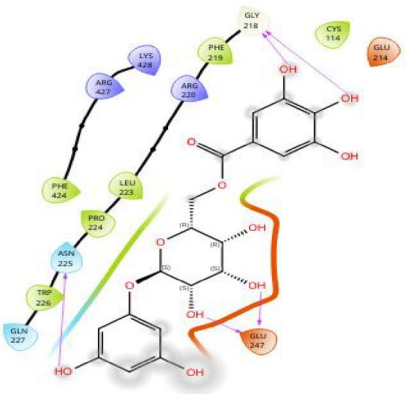
Lucidenic Acid A (14109375)	-7.305	-49.039	HSP90AA1	H bond: GLY 97 Polar: ASN 51, SER 52, HIE 154, THR 184 Glycine: GLY 97 Charged positive: LYS 58 Charged negative: ASP 54, ASP 93 Hydrophobic: LEU 48, ALA 55, ILE 91, ILE 96, MET 98, ALA 107, PHE 138, VAL 150, VAL 186	
7-hydroxycoumarin (5281426)	-4.262	-64.213	ICAM1	H bond: TYR L:94, LYS M: 65, SER A:417, THR A:389 GLN A:388, TRP A:382 Polar: GLN M:62, SER A:417, SER M:59, SER M: 58, THR A;389,GLN A:388, GLN A:387, THR A:381 Charged positive: LYS M:61, LYS M:65, Charged negative: ASP L:1 Hydrophobic: TRP H:47, TYR H:60, VAL L:93, TRP L:94, PRO L:95 TRP A:380, TRP A:382, PRO A:383, LEU A:448	
7-hydroxycoumarin (5281426)	-9.178	-66.777	IKBKB	H bond: GLY 218, ASN 225, GLU 247 Polar: ASN 225, GLN 227 Glycine: GLY 218 Charged positive: ARG 220, ARG 427, LYS 428 Charged negative: GLU 214, GLU 247 Hydrophobic: CYS 114, PHE 219, LEU 223, PRO 224, TRP 226, PHE 424	

Table 3 (continued)

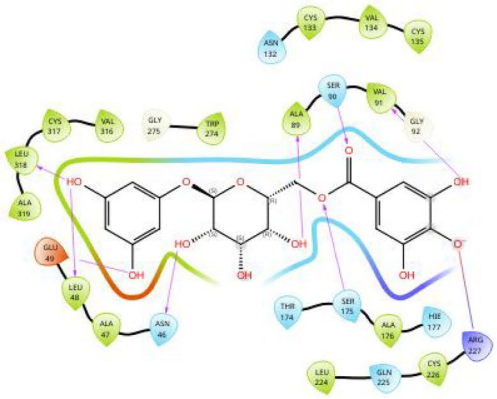
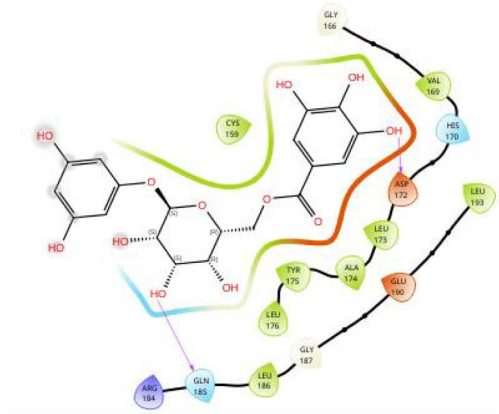
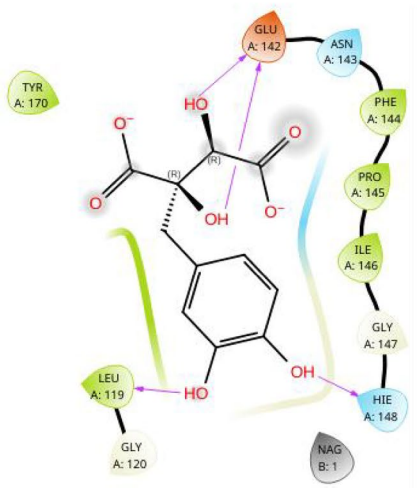
7-hydroxycoumarin (5281426)	-9.891	-82.213	MTOR	H Bond: ASN 46, LEU 48, GLU 49, LEU 318, ALA 89, SER 90, VAL 91, SER 175, ARG 227 Polar: ASN 46, SER 90, ASN 132, THR 174, SER 175, HIE 177, GLN 225 Glycine: GLY 92, GLY 275 Charged positive: ARG 227 Charged negative: GLU 49 Hydrophobic: ALA 47, LEU 48, ALA 89, ALA 91, CYS 133, VAL 134, CYS 135, ALA 176, LEU 224, CYS 226, TRP 274, VAL 316, CYS 317, LEU 318, ALA 319	
7-hydroxycoumarin (5281426)	-7.725	-67.955	NFKB1	H bond: ASP 172, GLN 185 Polar: HIS 170, GLN 185 Glycine: GLY 166, GLY 187 Charged positive: ARG 184 Charged negative: ASP 172, GLU 190 Hydrophobic: VAL 169, LEU 173, ALA 174, TYR 175, LEU 176, CYS 159, LEU 193, LEU 186	
Lathyrine (166766)	-6.522	-29.542	TLR4	H bond: LEU A:119, GLU A:142, HIE A:148 Polar: ASN A:143, HIE A:148 Glycine: GLY A:120, GLY A:147 Charged negative: GLU A:142 Metal: NAG B:1 Hydrophobic: LEU A:119, PHE A:144, PRO A:145, ILE A:146, TYR A:170	

Table 3 (continued)

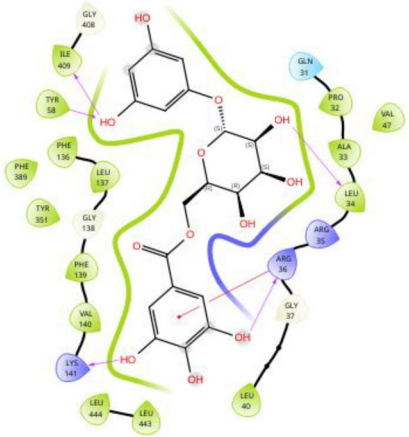
7-hydroxycoumarin (5281426)	-9.613	-96.863	TNF	H bond: LEU 34, ARG 36, LYS 141, TYR 58, ILE 409 Pi cation: ARG 36 Polar: GLN 31 Glycine: GLY 138, GLY 37, GLY 408 Charged positive: ARG 35, ARG 36, LYS 141 Hydrophobic: PRO 32, ALA 33, LEU 34, LEU 40, VAL 47, TYR 58, PHE 136, LEU 137,PHE 139,VAL 140, TYR 351, PHE 389, ILE 409,LEU 443, LEU 444	

Table 4 Disc diffusion assay of *A. calamus* root extracts from different cultivation systems on different bacterial strains

Bacterial Pathogen	Extracts used	Concentration of extracts (µg/ml)	Volume (µL)	Zone of Inhibition (mm)	Positive control	Significance
Pseudomonas aeruginosa	Soil	2000	20	27.3±2.5	23±0.8	>0.05
	Hydroponic	2000	20	27±2.44	23±0.8	>0.05
Staphylococcus aureus	Soil	2000	20	18.3±2.8	15.3±0.4	>0.05
	Hydroponic	2000	20	16.6±2.05	15.6±0.4	>0.05
Streptococcus mutans	Soil	2000	20	17±1.63	17.6±0.4	>0.05
	Hydroponic	2000	20	17±2.4	17.3±0.4	>0.05
Enterococcus faecalis	Soil	2000	20	16.6±0.94	14.3±0.4	$<0.05^{*}$
	Hydroponic	2000	20	18.3±0.47	14.6±0.4	$<0.001^{***}$

All values are represented as (mean±SD); * $p<0.05$, ** $p<0.01$, *** $p<0.001$

research has focused on the plant's rhizome, this study highlights the roots of *A. calamus* as an underexplored reservoir of secondary metabolites with promising therapeutic potential. Our findings reveal that growth parameters, including plant height, leaf biomass, and root biomass, are significantly higher in hydroponically grown *A. calamus* than in soil-grown plants. These results are consistent with earlier studies reporting enhanced growth performance in hydroponically cultivated medicinal and food crops (Chamoli et al. 2024; Surendran et al. 2016). The growth of the plant is directly linked to the photosynthetic process (Fonseca et al. 2022). In our study, the photosynthetic rate during weeks 2 and 4 may be attributed to the efficient carbon dioxide uptake and high catalytic activity of the Rubisco enzyme (Opoku et al. 2024; Yang et al. 2024). However, the decline in photosynthetic rate during the later growth phase may be attributed to root restriction and oxygen deficiency (Pezeshki and Santos 1998).

Metabolomic analysis revealed distinct differences between the cultivation systems, highlighting the substantial impact of the growth and environmental conditions on biosynthetic pathways (Ai et al. 2021; Nazarideljou 2023). Hydroponic roots showed the accumulation of key pharmacologically relevant metabolites, including allantoin and 3,5-Dihydroxyphenyl. Furthermore, they exhibited enhanced production of antioxidant compounds, including 6-(5-carboxy-2,3-dihydroxyphenoxy)−3,4,5-trihydroxyoxane-2-carboxylic acid, and alkaloids with antimicrobial properties, such as allantoin, graveoline, and capnoidine. Graveoline exhibits exceptional antimicrobial property, with notable effectiveness against *S. aureus* and *E. faecalis* (MIC 500–1000 µg/mL) (Mohd Kamal et al. 2018). Allantoin serves as another important contributor to the antibacterial profile through its low MIC values (4–8 µg/mL) against Gram-positive bacteria (Lakshmanan et al. 2019). Together, these findings suggest that hydroponic systems may provide a reliable platform for enhancing yields of antimicrobial and antioxidant compounds.

In contrast, soil-grown plants exhibited higher levels of metabolites like triphenyl phosphate and

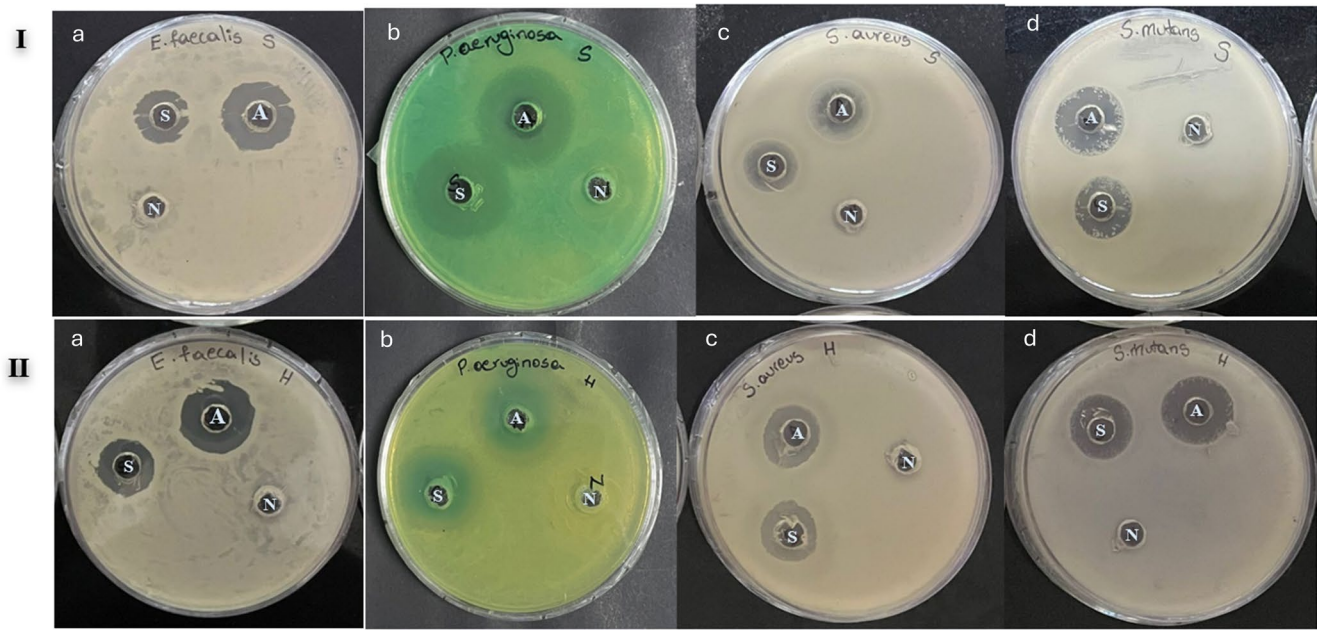


Fig. 7 Antibacterial activity of *A. calamus* extracts against different bacterial pathogens. Zones of inhibition produced against (**a**) *Enterococcus faecalis*, (**b**) *Pseudomonas aeruginosa*, (**c**) *Staphylococcus aureus*, *and* (**d**) *Streptococcus mutans;* (I) Soil and (II) Hydroponic cultivation. The control treatments include (A) Ciprofloxacin (antibiotic), (N) 10% DMSO as a negative control, and (S) represents the *A. calamus* plant extract used in the assay (2000 µg/ml)

3,5-dihydroxyphenyl 1-O-(6-O-galloyl-beta-D-glucopyranoside), compounds associated with stress-responsive pathways, consistent with patterns observed in soybeans and lettuce under field conditions (Wimmerova et al. 2022). This divergence suggests that hydroponic cultivation provides a more conducive environment for the biosynthesis of targeted bioactive compounds with pharmacological relevance, while soil cultivation triggers stress-adaptive metabolic responses. This highlights the potential of hydroponic systems not only for sustainable production but also for enhancing the quality of medicinal plants by modulating environmental factors that influence metabolic pathways.

Network pharmacology analysis further demonstrated that hydroponically grown *A. calamus* metabolites engage multiple bacterial defence and virulence pathways. The identification of hub targets, including TL4, MTOR, TNF, NFKB1, CASP1, and ICAM1, suggests that these metabolites interact with key regulatory nodes involved in inflammation and immune defence. Further, the molecular docking analysis of 59 ligands against the 10 hub protein targets revealed notably strong binding affinities for TNF (−12.94 kcal/mol), MTOR (−11.6 kcal/mol), and ICAM1 (−10.51 kcal/mol). Because more negative docking scores indicate stronger ligand-protein interactions, TNF and MTOR emerge as particularly favourable targets, with affinities comparable to those reported for established pharmacological inhibitors (Khan and Lee 2023; Patidar et al. 2019). The strong TNF interaction is notable because TNF-α is a central pro-inflammatory mediator and validated therapeutic target. Likewise, high MTOR affinity aligns with potential antibacterial effects, as MTOR regulates immune metabolism, autophagy-mediated bacterial clearance, and cytokine production. Although BCL2 showed only moderate affinity, it may still be relevant since pathogens often exploit BCL2-mediated cell survival to support intracellular replication (Chen et al. 2024). These findings collectively suggest that the identified metabolites may act through a multi-target mechanism, exerting their antimicrobial and antioxidant effects.

Consistent with these predictions, the antibacterial assays demonstrated that hydroponic *A. calamus* extracts exhibit robust inhibition across all four clinically important pathogens tested, with inhibition zone diameters of 24–30 mm (*P. aeruginosa*), 14–19 mm (*S. aureus*), 14–20 mm (*S. mutans*), and 18–19 mm (*E. faecalis*). The hydroponic extracts showed slightly greater inhibition of *P. aeruginosa*, *E. faecalis*, *S. aureus*, and *S. mutans* than the soil extracts.

Overall, hydroponic cultivation enhances the yield and therapeutic potential of bioactive metabolites, enabling multi-pathway antibacterial activity. These findings position hydroponics as a promising strategy for producing medicinal plant extracts with optimised antibacterial efficacy. This study highlights the significant impact of cultivation methods on the metabolite profiles, physiological characteristics, and pharmacological potential of *A. calamus*. Hydroponic systems offer controlled environments

that enhance the production of bioactive metabolites, promote sustainable farming by reducing dependence on soil resources, and help mitigate the pressures of over-harvesting. In contrast, soil-based cultivation favours the synthesis of stress-related metabolites, reflecting the plant's adaptive responses to fluctuating field conditions. These findings offer valuable insights for sustainable agriculture and ethnopharmacology, paving the way for more in-depth investigations into the molecular mechanisms underlying these variations and the potential for scaling up hydroponic cultivation.

5 Conclusion

This study emphasises the significant influence of cultivation methods on the metabolomic profiles and therapeutic potential of *A. calamus*, comparing hydroponic and soil-based systems. By linking physiological and metabolomic changes to antibacterial outcomes, our work not only identifies A. calamus root as an underexplored reservoir of therapeutic compounds but also provides a sustainable framework for cultivating medicinal plants that optimises metabolite synthesis, reduces ecological impact, and supports urban farming. Future studies should investigate the molecular mechanisms driving these metabolic variations and evaluate the economic feasibility of large-scale hydroponic production. Integrating hydroponics with precision agriculture technologies could further enhance efficiency, scalability, and sustainability, strengthening its role in advancing medicinal plant cultivation and ethnopharmacology.

Acknowledgements The authors are thankful to the Manipal Academy of Higher Education, Manipal, India, and DBT-BUILDER (Ref. BT/INF/22/SP43065/2021), Govt. of India, and Department of Science and Technology (DST)-FIST (SR/FST/LS-II/2018/240), Government of India, for developing the infrastructure and facilities at Manipal School of Life Sciences. The authors would also like to thank Dr. TMA Pai, PhD Scholarship, and Council of Scientific and Industrial Research (CSIR) SRF-Direct fellowship, Government of India (181-969-2189/2K23/1).

Author Contributions **Andrew D'Souza**: Data curation, Formal analysis, Investigation, Software, Visualization, Writing – original draft, Data Interpretation. **Kannath U Sanjay**: Formal analysis, Investigation, Data Interpretation, Writing – original draft. **Neeharika Narisepalli Venkatasai**: Data curation, Formal analysis, Investigation, Software visualisation. **Padmalatha S Rai**: Conceptualisation, Formal analysis, Writing– review & editing, Project administration, Supervision.

Funding Open access funding provided by Manipal Academy of Higher Education, Manipal.

Data Availability Data will be made available on request.

Declarations

Ethical Statements This research article does not contain any studies with human or animal participants.

Conflict of Interest The authors declare that they have no conflicts of interest, financial or otherwise.

Open Access This article is licensed under a Creative Commons Attribution 4.0 International License, which permits use, sharing, adaptation, distribution and reproduction in any medium or format, as long as you give appropriate credit to the original author(s) and the source, provide a link to the Creative Commons licence, and indicate if changes were made. The images or other third party material in this article are included in the article's Creative Commons licence, unless indicated otherwise in a credit line to the material. If material is not included in the article's Creative Commons licence and your intended use is not permitted by statutory regulation or exceeds the permitted use, you will need to obtain permission directly from the copyright holder. To view a copy of this licence, visit http://creativecommons.org/licenses/by/4.0/.

References

Ai P, Liu X, Li Z, Kang D, Khan MA, Li H, Shi M, Wang Z (2021) Comparison of chrysanthemum flowers grown under hydroponic and soil-based systems: yield and transcriptome analysis. BMC Plant Biol 21:517. https://doi.org/10.1186/s12870-021-03255-4

Atherton HR, Li P (2023) Hydroponic cultivation of medicinal plants—plant organs and hydroponic systems: techniques and trends. Horticulturae 9:349. https://doi.org/10.3390/horticulturae9030349

Burley SK, Bhikadiya C, Bi C et al (2021) RCSB protein data bank: powerful new tools for exploring 3D structures of biological macromolecules for basic and applied research and education in fundamental biology, biomedicine, biotechnology, bioengineering and energy sciences. Nucleic Acids Res 49:D437–D451. https://doi.org/10.1093/nar/gkaa1038

Chamoli N, Kumar M, Das S, Prabha D, Chauhan JS (2024) Comparative analysis of hydroponically and soil-grown lettuce. J Mt Res 19:583–591. https://doi.org/10.51220/jmr.v19-i2.61

Chen H, Chen E, Liu M, Wang J, Yin J, Zhao P, Xu Y (2024) Identification of immune-related endoplasmic reticulum stress genes in proliferative diabetic retinopathy using bioinformatics analysis. Front Endocrinol 15:1341206. https://doi.org/10.3389/fendo.2024.1341206

De Vos RCH, Moco S, Lommen A, Keurentjes JJB, Bino RJ, Hall RD (2007) Untargeted large-scale plant metabolomics using liquid chromatography coupled to mass spectrometry. Nat Protoc 2:778–791. https://doi.org/10.1038/nprot.2007.95

Fonseca M, da deC, Bossolani JW, de Oliveira SL et al (2022) Bacillus subtilis inoculation improves nutrient uptake and physiological activity in sugarcane under drought stress. Microorganisms 10:809. https://doi.org/10.3390/microorganisms10040809

Haran P, Shanmugam R, Deenadayalan P (2024) Free radical scavenging, anti-inflammatory and antibacterial activity of *Acorus calamus* leaves extract against *Pseudomonas aeruginosa* and *Staphylococcus aureus*. Cureus 16:e55987. https://doi.org/10.7759/cureus.55987

He X, Chen X, Yang Y, Liu Y, Xie Y (2023) *Acorus calamus* var. *angustatus* Besser: insight into current research on ethnopharmacological use, phytochemistry, pharmacology, toxicology, and

pharmacokinetics. Phytochemistry 210:113626. https://doi.org/10.1016/j.phytochem.2023.113626
Jilani MR, Packirisamy ASB (2024) Terpenoids and fatty acid esters from underutilized tiliaceae shrub exhibit in silico bioactivity and protein targets. Top Catal 67:74–85. https://doi.org/10.1007/s11244-023-01862-z
Jumper J, Evans R, Pritzel A et al (2021) Highly accurate protein structure prediction with AlphaFold. Nature 596:583–589. https://doi.org/10.1038/s41586-021-03819-2
Kaur S, Dewan B (2023) Hydroponics: a review on revolutionary technology for sustainable agriculture. Asian J Agric Hortic Res 10:297–302. https://doi.org/10.9734/ajahr/2023/v10i4270
Khan SA, Lee TKW (2023) Identifying potential pharmacological targets and molecular pathways of Meliae cortex for COVID-19 therapy. Front Immunol 14:1128164. https://doi.org/10.3389/fimmu.2023.1128164
Kim M, Nowakowska A, Kim J, Kim YB (2024) Anti-influenza a potential of *Tagetes erecta* Linn. extract based on bioinformatics analysis and in vitro assays. Int J Mol Sci 25:7065. https://doi.org/10.3390/ijms25137065
Kontoyianni M (2017) Docking and Virtual Screening in Drug Discovery. In: Lazar IM, Kontoyianni M, Lazar AC (eds) Proteomics for Drug Discovery. Springer New York, New York, NY, pp 255–266
Lakshmanan G, Sivaraj C, Ammar A, Anantha Krishnan D et al (2019) Isolation and structural Elucidation of Allantoin a bioactive compound from cleome viscosa L A combined experimental and computational investigation. Pharmacogn J 11:1391–1400. https://doi.org/10.5530/pj.2019.11.215
Liu S, He C, Liao Y, Liu H, Mao W, Shen Z (2020) Enhancing and complementary mechanisms of synergistic action of *Acori tatarinowii* rhizoma and *Codonopsis radix* for Alzheimer's disease based on systems pharmacology. Evid Based Complement Alternat Med 2020:6317230. https://doi.org/10.1155/2020/6317230
Mohd Kamal LZ, Mohd Hassan N, Md Taib N, May KS (2018) Graveoline from Ruta angustifolia (L.) Pers. and its antimicrobial synergistic potential in erythromycin or Vancomycin combinations. Sains Malays 47:2429–2435. https://doi.org/10.17576/jsm-2018-4710-19
Nazarideljou MJ (2023) Biomass and volatile compounds of rose-scented geranium under various elicitors and cultivation systems. J Essent Oil-Bear Plants 26:987–1007. https://doi.org/10.1080/0972060X.2023.2258535
Opoku E, Sahu PP, Findurová H, Holub P, Urban O, Klem K (2024) Differential physiological and production responses of C3 and C4 crops to climate factor interactions. Front Plant Sci 15:1345462. https://doi.org/10.3389/fpls.2024.1345462
Pang Z, Lu Y, Zhou G, Hui F, Xu L, Viau C, Spigelman AF, MacDonald PE, Wishart DS, Li S, Xia J (2024) MetaboAnalyst 6.0: towards a unified platform for metabolomics data processing, analysis and interpretation. Nucleic Acids Res 52:W398–W406. https://doi.org/10.1093/nar/gkae253
Patidar K, Panwar U, Vuree S, Sweta J, Sandhu MK, Nayarisseri A, Singh SK (2019) An in Silico approach to identify high-affinity small molecule targeting m-TOR inhibitors for the clinical treatment of breast cancer. Asian Pac J Cancer Prev 20:1229–1241. https://doi.org/10.31557/APJCP.2019.20.4.1229
Pezeshki SR, Santos MI (1998) Relationships among rhizosphere oxygen deficiency, root restriction, photosynthesis, and growth in Baldcypress (*Taxodium distichum* L.) seedlings. Photosynthetica 35:381–390. https://doi.org/10.1023/A:1006912318352
Prasathkumar M, Anisha S, Dhrisya C, Becky R, Sadhasivam S (2021) Therapeutic and pharmacological efficacy of selective Indian medicinal plants – a review. Phytomedicine Plus 1:100029. https://doi.org/10.1016/j.phyplu.2021.100029
Rajput SB, Tonge MB, Karuppayil SM (2014) An overview on traditional uses and pharmacological profile of *acorus calamus* Linn. (Sweet flag) and other *acorus* species. Phytomedicine 21:268–276. https://doi.org/10.1016/j.phymed.2013.09.020
Regmi S, Neupane S (2023) Possible sustainable agricultural practices in nepal: A review. Agr Ext Dvp Ctries 1:62–66. https://doi.org/10.26480/aedc.02.2023.62.66
Sahu T, Vedantam G, Vetrivel U (2024) In silico exploration of bioactive compounds from *acorus calamus* L. for targeted treatment of ischemic heart disease: molecular insights and therapeutic prospects. J Drug Res Ayurvedic Sci 9:150. https://doi.org/10.4103/jdras.jdras_104_23
Surendran U, Chandran C, Joseph EJ (2016) Hydroponic cultivation of mentha spicata and comparison of biochemical and antioxidant activities with soil-grown plants. Acta Physiol Plant 39:26. https://doi.org/10.1007/s11738-016-2320-6
Szklarczyk D, Gable AL, Lyon D, Junge A, Wyder S, Huerta-Cepas J, Simonovic M, Doncheva NT, Morris JH, Bork P, Jensen LJ, von Mering C (2019) STRING v11: protein–protein association networks with increased coverage, supporting functional discovery in genome-wide experimental datasets. Nucleic Acids Res 47:D607–D613. https://doi.org/10.1093/nar/gky1131
Thorat SA, Srivaishnavi M, Kaniyassery A, Chandrashekar HK, Mahato KK, Muthusamy A (2024) He-Ne laser pre-exposure alleviates salinity stress through physio-biochemical regulation and enhanced withanolide production in Withania somnifera (L.) Dunal. Ind Crop Prod 216:118776. https://doi.org/10.1016/j.indcrop.2024.118776
Tiwari KL, Jadhav SK, Gupta S (2012) Modified CTAB technique for isolation of DNA from some medicinal plants. Res J Med Plant 6:65–73. https://doi.org/10.3923/rjmp.2012.65.73
Vinay CM, Shetty DN, Sanjay KU, Venkatasai NN, Rai PS (2025) Impact of Salicylic acid elicitation on the growth, photosynthesis, and metabolites of Bacopa monnieri (L.) Pennell growing in a hydroponic control system. Sci Hortic 342:114056. https://doi.org/10.1016/j.scienta.2025.114056
Wimmerova L, Keken Z, Solcova O, Bartos L, Spacilova M (2022) A comparative LCA of aeroponic, hydroponic, and soil cultivations of bioactive substance producing plants. Sustainability 14:2421. https://doi.org/10.3390/su14042421
Yang R, Yang H, Ji F, He D, Yang R, Yang H, Ji F, He D (2024) Enhancing the photon yield of hydroponic lettuce through stage-wise optimization of the daily light integral in an LED plant factory. Agronomy 14:2949. https://doi.org/10.3390/agronomy14122949

Publisher's Note Springer Nature remains neutral with regard to jurisdictional claims in published maps and institutional affiliations.